Electron screening: answer to an old problem from a new perspective

Aleksandra Cvetinović

Jožef Stefan Institute, Ljubljana

19th Rußbach School on Nuclear Astrophysics

Rußbach, March 2024

Introduction:

How were the chemical elements created?

- The only way to answer this question is to **study nuclear reactions at energies within the Gamow window**.
- Knowing reaction probabilities at these energies accurately will allow us to learn more about the nucleosynthesis and internal processes happening in stars.

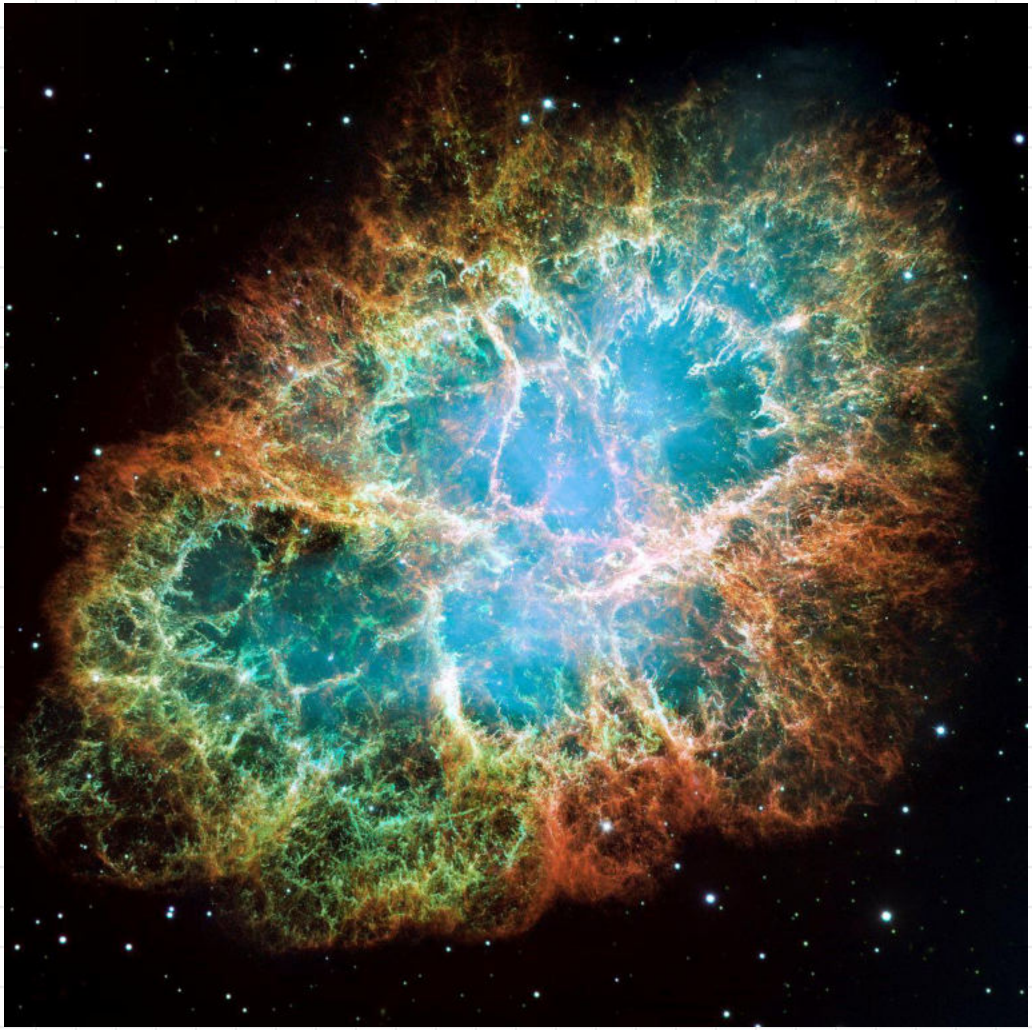

Introduction:

Nuclear Reactions at the Gamow window

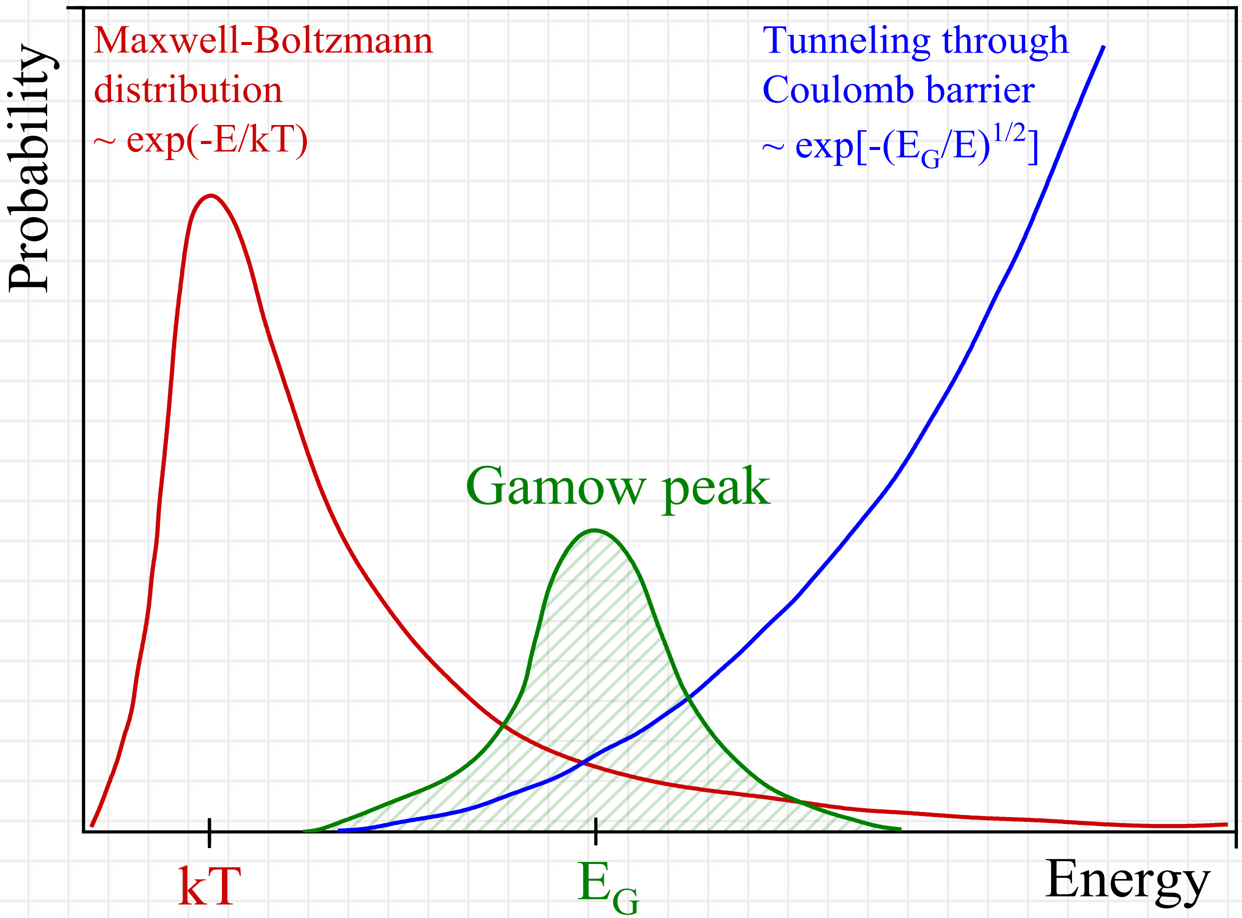

3-30 keV for stellar hydrogen-burning reactions in the cores of main sequence stars

~300 keV for stellar helium-burning reactions in the cores of red giant stars

1-2 MeV for stellar carbon burning

Introduction:

Nuclear Reactions at the Gamow window

- In nuclear reactions between charged particles at low energies, when the energy of the incident beam in the center of mass system is far below the Coulomb barrier, tunneling is the only way the fusion process can happen.

The probability that an incoming particle penetrates the Coulomb barrier:

$$T = \frac{|\Psi_{R_n}|^2}{|\Psi_{R_C}|^2}$$

$$T \approx exp\left\{-\frac{2}{\hbar}\sqrt{\frac{2\mu}{E}}Z_0 Z_1 e^2\left[arccos\sqrt{\frac{E}{V_C}} - \sqrt{\frac{E}{V_C}}\left(1-\frac{E}{V_C}\right)\right]\right\}$$

when $E/V_C \ll 1$:

$$T \approx exp\left\{-\frac{2}{\hbar}\sqrt{\frac{2\mu}{E}}Z_0 Z_1 e^2\left[\frac{\pi}{2} - 2\sqrt{\frac{E}{V_C}} + \frac{1}{3}\left(\frac{E}{V_C}\right)^{3/2}\right]\right\}$$

$$= exp\left\{-\frac{2\pi}{\hbar}\sqrt{\frac{\mu}{2E}}Z_0 Z_1 e^2\left[1 + \frac{2}{3\pi}\left(\frac{E}{V_C}\right)^{3/2}\right] + \frac{4}{\hbar}\sqrt{2\mu Z_0 Z_1 e^2 R_n}\right\}$$

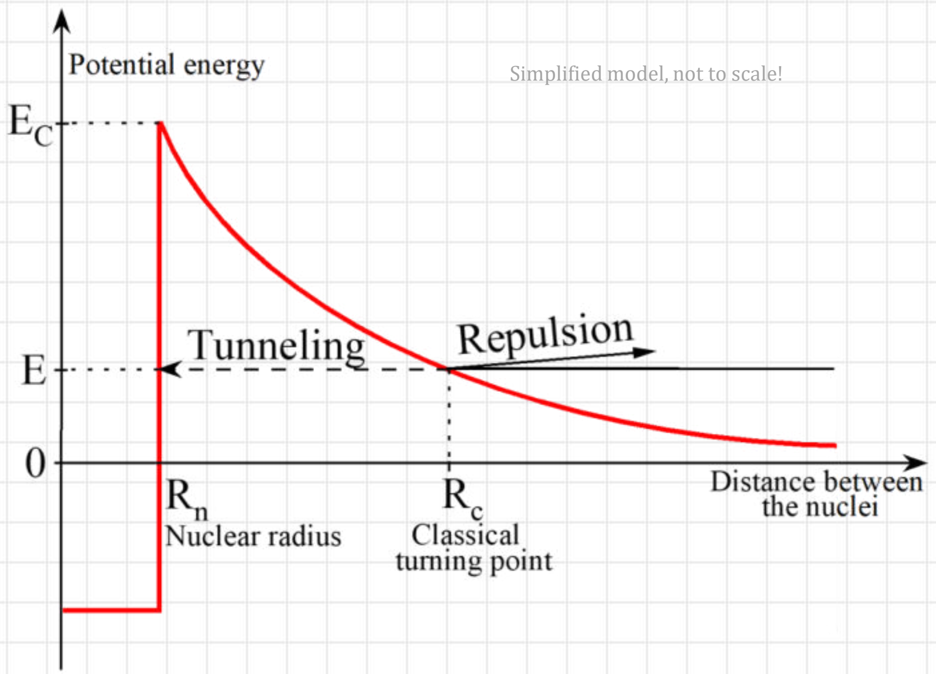

C. Iliadis, Nuclear Physics of Stars - Second, Revised and Enlarged Edition, Wiley-VCH, Weinheim, 2015.

Introduction:

Nuclear Reactions at the Gamow window

Sommerfeld parameter:
$\eta = Z_1 Z_2 e^2 / 4\pi\varepsilon_o \hbar (2E/\mu)^{1/2}$

Gamow factor:

$G = \exp\left(-2\pi\eta(E)\right)$ - describes the s-wave penetration through the Coulomb barrier of point like charges

Cross section:

$\sigma(E) = S(E)E^{-1}\exp\left(-2\pi\eta(E)\right)$

E – geometrical factor

Astrophysical *S*-factor:

$S(E)$ **-** contains all nuclear effects and in the case of non-resonant reactions **varies smoothly with energy**

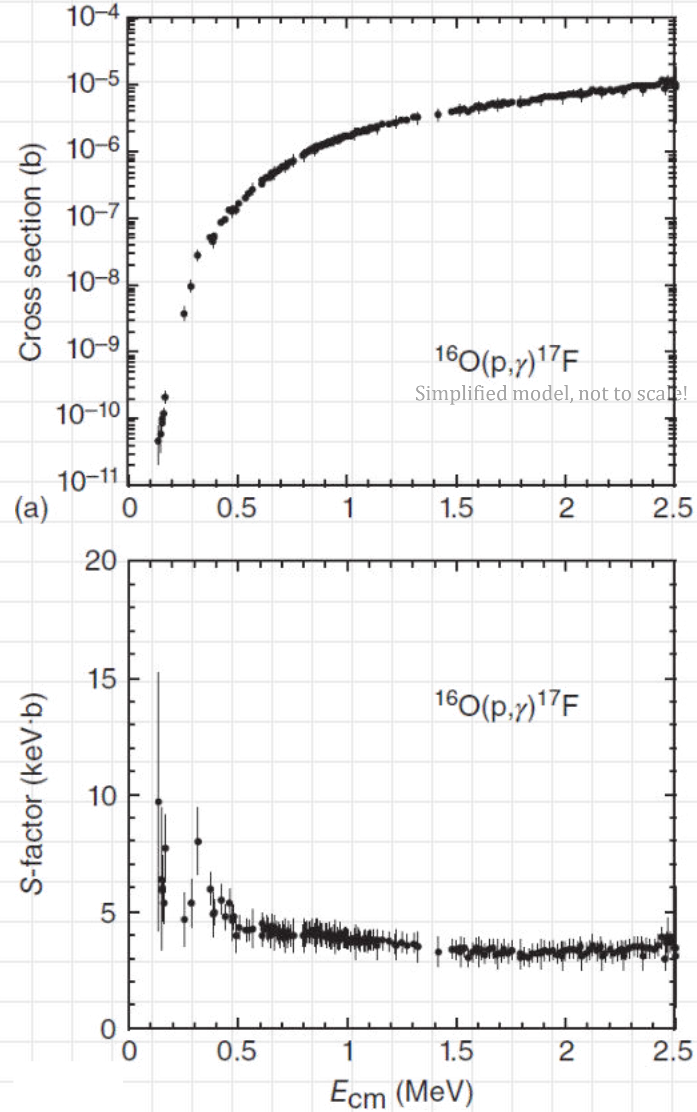

C. Iliadis, Nuclear Physics of Stars - Second, Revised and Enlarged Edition, Wiley-VCH, Weinheim, 2015.

Nuclear Reactions at the Gamow window

- When the tunneling effect is the only way for the reaction to happen, the probability for fusion drops steeply with decreasing beam energy because of the huge repulsive Coulomb barrier through which the projectile has to penetrate.
- The cross sections at energies in the astrophysical region are extremely difficult to measure.

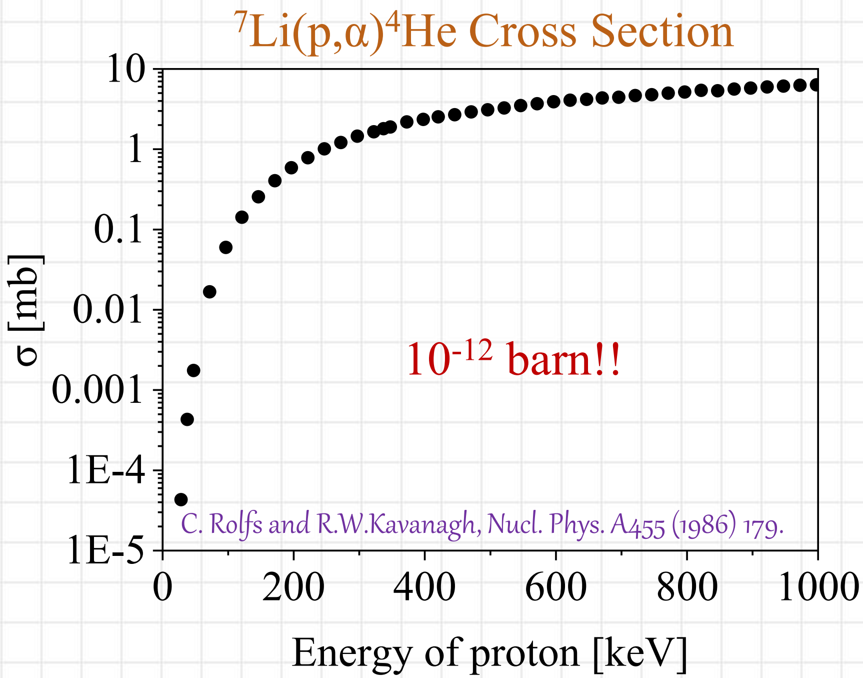

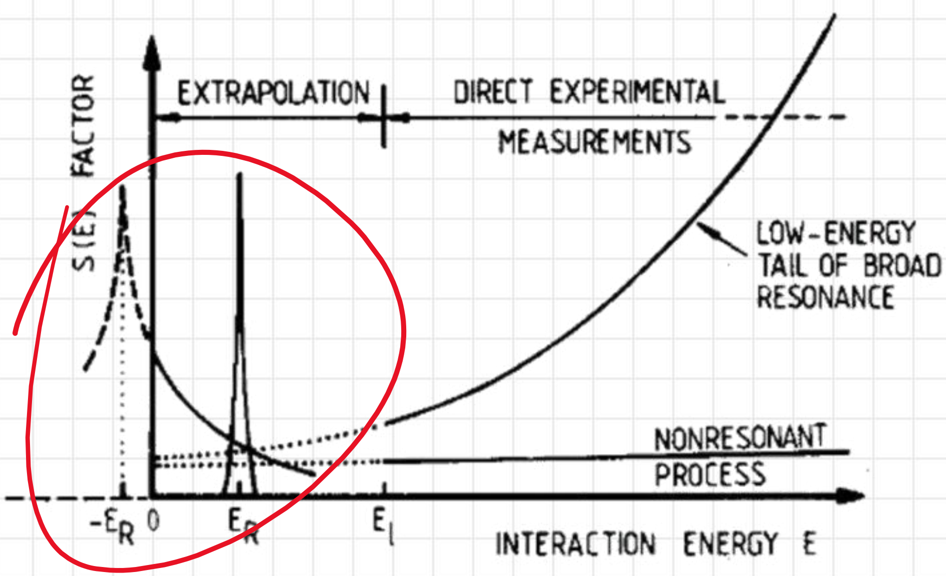

[1] A. B. Balantekin et al. Nucl. Phys. A, 627 (1997) 324.

Electron Screening Effect

- Accurate measurements of nuclear reactions induced by low-energy charged particles, show an unexpectedly **large enhancement of the cross section** in Gamow energy region, that is attributed to the **presence of atomic electrons.**

Adiabatic Model:

- *Employs a static approximation*
- *Assumes unchanged electron density between interacting nuclei*
- $V_{nucleus} << V_{e\_orb}$
- *Upper theoretical limit for Ue :*

  Adiabatic limit in a static approximation

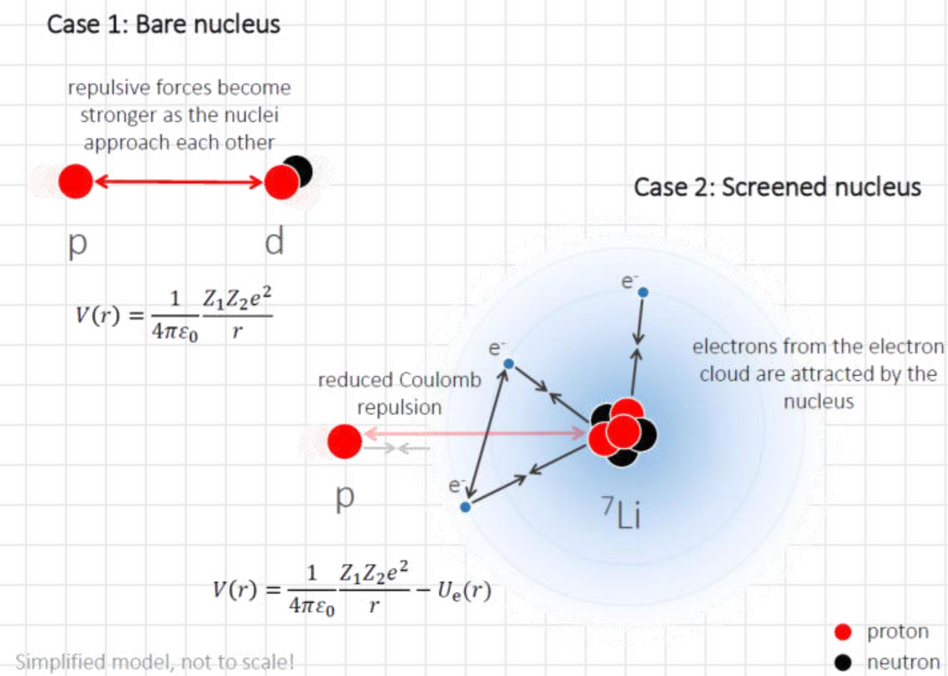

- Atomic and nuclear polarizabilities, vacuum polarization, electron excitations or relativistic effects lead to a **lower value of the screening potential**[1].

[1] A. B. Balantekin et al. Nucl. Phys. A, 627 (1997) 324.

Electron Screening Effect

- Accurate measurements of nuclear reactions induced by low-energy charged particles, show an unexpectedly **large enhancement of the cross section** in Gamow energy region, that is attributed to the **presence of atomic electrons.**

Adiabatic Model:

- *Employs a static approximation*
- *Assumes unchanged electron density between interacting nuclei*
- $V_{nucleus} << V_{e\_orb}$
- *Upper theoretical limit for Ue :*

  Adiabatic limit in a static approximation

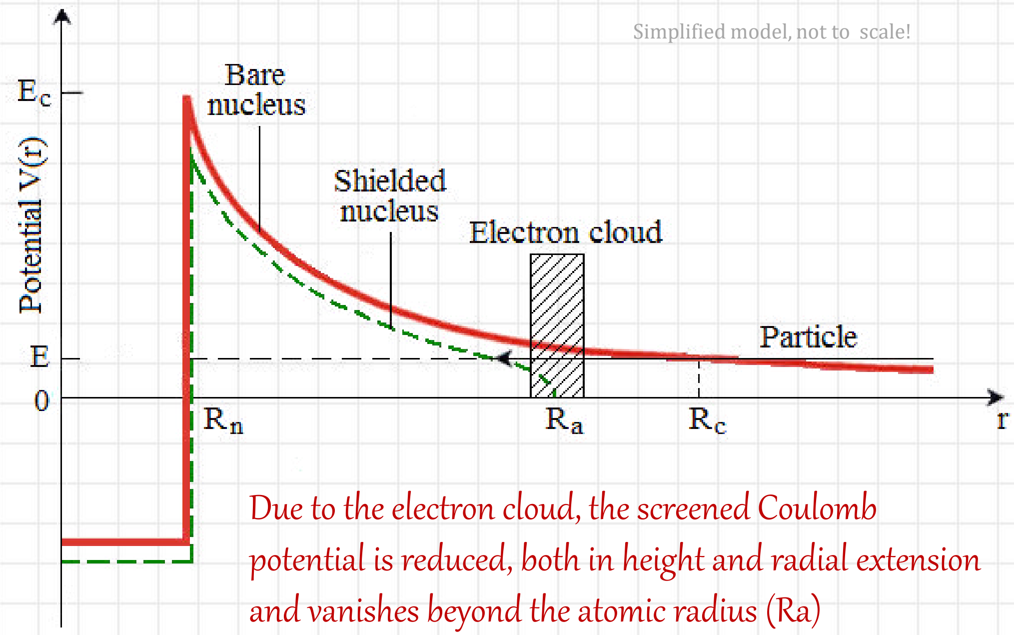

Due to the electron cloud, the screened Coulomb potential is reduced, both in height and radial extension and vanishes beyond the atomic radius (Ra)

- Atomic and nuclear polarizabilities, vacuum polarization, electron excitations or relativistic effects lead to a **lower value of the screening potential**[1].

[1] H. J. Assenbaum, K. Langanke and C. Rolfs, Z. Phys. A 327 (1987) 461.
[2] C. A. Bertulani et al, J. Phys.: Conf. Ser. 703 (2016) 012007.

Electron Screening Effect

- When astrophysical energies are reached in underground laboratories, measurements do not give the bare-nucleus cross section, but we measure the screened one.
- **Then, how do we take into account the screening effect?**

Enhancement factor:

$$f(E) = \frac{\sigma_s(E+U_e)}{\sigma_b(E)} = \frac{e^{-2\pi\eta(E+U_e)}}{e^{-2\pi\eta(E)}}$$

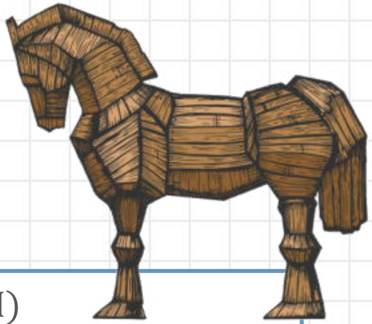

[2]

Trojan Horse Method (THM)
Asymptotic Normalization Coefficient (ANC)
Coulomb dissociation method (CD)
Surrogate and charge-exchange reactions

Upper theoretical limit from adiabatic model in a static approximation:

$$U_e = \frac{Z_1 Z_2 e^2}{4\pi\varepsilon_0 R_a} = 27 \text{ eV}$$ for d+d reaction![1]

- ***Many experimental results showed significant disagreement with the theory!***

Previous Results

- With gaseous targets, obtained screening potentials are in agreement with the adiabatic limit.
- With the target nucleus implanted in a solid lattice, obtained screening potentials are much above the adiabatic limit

Material	U_e (eV)[b]	Solubility $1/x$ [c]	n_{eff} [b]
		Metals	
Be	180±40	0.08	0.2±0.1
Mg	440±40	0.11	3.0±0.5
Al	520±50	0.26	3.0±0.6
V	480±60	0.04	2.1±0.5
Cr	320±70	0.15	0.8±0.4
Mn	390±50	0.12	1.2±0.3
Fe	460±60	0.06	1.7±0.4
Co	640±70	0.14	3.1±0.7
Ni	380±40	0.13	1.1±0.2
Cu	470±50	0.09	1.8±0.4
Zn	480±50	0.13	2.4±0.5
Sr	210±30	0.27	1.7±0.5
Nb	470±60	0.13	2.7±0.7
Mo	420±50	0.12	1.9±0.5
Ru	215±30	0.18	0.4±0.1
Rh	230±40	0.09	0.5±0.2
Pd	800±90	0.03	6.3±1.3
Ag	330±40	0.14	1.3±0.3
Cd	360±40	0.18	1.9±0.4
In	520±50	0.02	4.8±0.9
Sn	130±20	0.08	0.3±0.1
Sb	720±70	0.13	11±2
Ba	490±70	0.21	9.9±2.9
Ta	270±30	0.13	0.9±0.2
W	250±30	0.29	0.7±0.2
Re	230±30	0.14	0.5±0.1
Ir	200±40	0.23	0.4±0.2
Pt	670±50	0.06	4.6±0.7
Au	280±50	0.18	0.9±0.3
Tl	550±90	0.01	5.8±1.2
Pb	480±50	0.04	4.3±0.9
Bi	540±60	0.12	6.9±1.5

Material	U_e (eV)[b]	Solubility $1/x$ [c]	n_{eff} [b]
		Semiconductors	
C	⩽ 60	0.35	
Si	⩽ 60	0.23	
Ge	⩽ 80	0.56	
		Insulators	
BeO	⩽ 30	0.25	
B	⩽ 30	0.38	
Al_2O_3	⩽ 30	0.27	
CaO_2	⩽ 50	0.60	
		Groups 3 and 4	
Sc	⩽ 30	1.4	
Ti	⩽ 30	1.3	
Y	⩽ 70	1.8	
Zr	⩽ 40	1.1	
Lu	⩽ 40	1.5	
Hf	⩽ 30	1.8	
		Lanthanides	
La	⩽ 60	0.6	
Ce	⩽ 30	1.3	
Pr	⩽ 70	0.9	
Nd	⩽ 30	0.7	
Sm	⩽ 30	1.3	
Eu	⩽ 50	0.6	
Gd	⩽ 50	1.4	
Tb	⩽ 30	1.3	
Dy	⩽ 30	1.1	
Ho	⩽ 70	1.6	
Er	⩽ 50	1.0	
Tm	⩽ 70	1.4	
Yb	⩽ 40	1.3	

$$\boxed{U_e^{ad} = 27 \text{ eV for } {}^2\text{H(d,p)3H}}$$

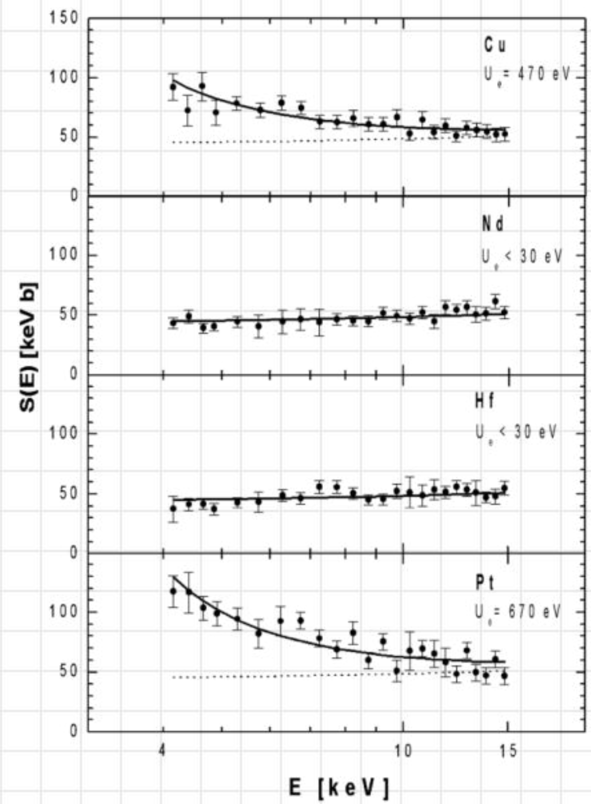

F. Raiola et al., Eur. Phys. J. A19 (2004) 283.

Previous Results

J. Cruz et al., Phys. Lett. B 624 (2005) 181

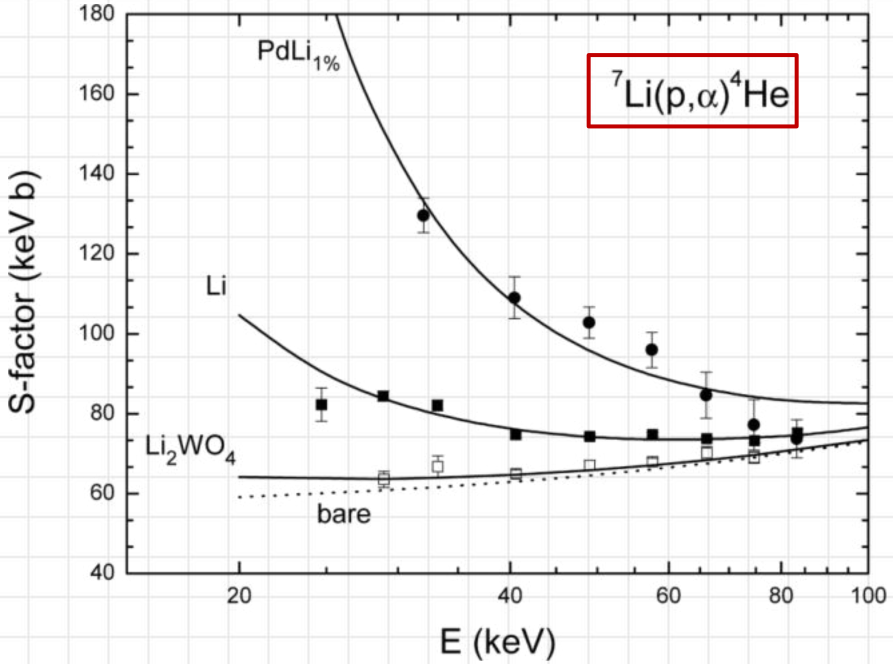

PdLi$_{1\%}$: Ue = 3.7±0.3 keV
Li metal: Ue = 1.18±0.06 keV
Li2WO4: Ue = 237^{+133}_{-77} eV

$^2H(d,p)3H$

J. Kasagi, Prog. Theo. Phys. Suppl. 154 (2004) 365.

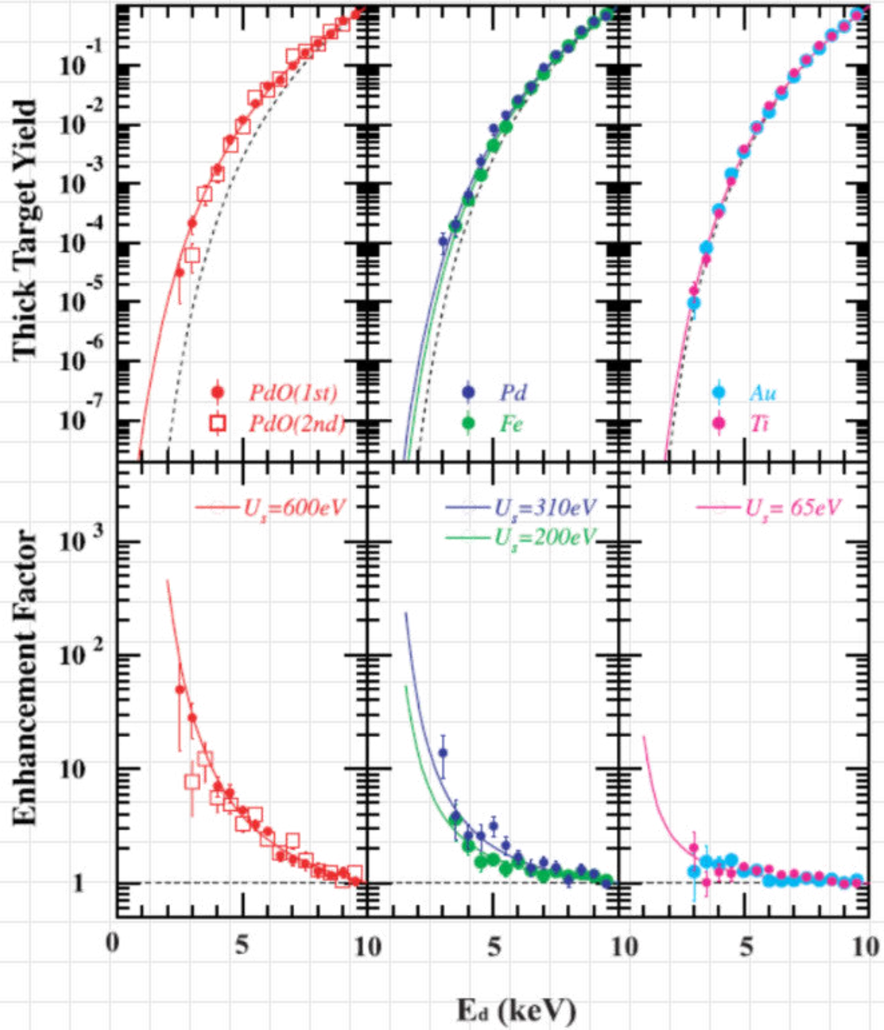

Previous Results

$\boxed{U_e^{ad} = 27 \text{ eV for } {}^2\text{H(d,p)3H}}$

F. Raiola et al., J. Phys. G 31, (2005) 1141.

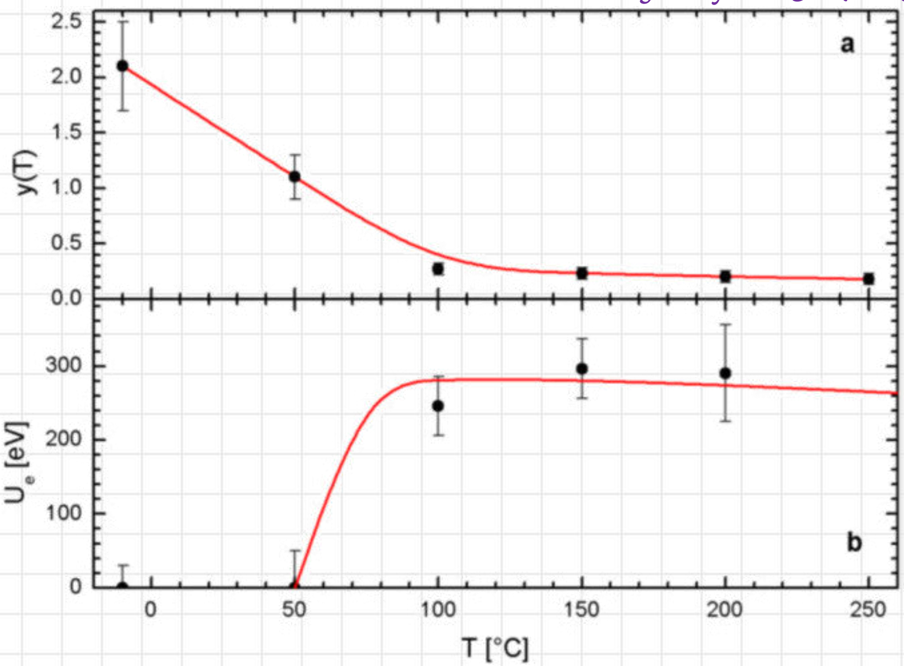

Hydrogen solubility y(T) and the screening potential Ue(T) in Ti as a function of sample temperature T.

Material	T (°C)	U_e (eV)[b]	Solubility y[c]	n_{eff}[b]
		T-dependence of Pt and Co		
Pt	20	675 ± 70	0.06	
	100	530 ± 40	0.06	
	200	530 ± 40	0.05	
	300	465 ± 38	0.04	
	340	480 ± 70	0.04	
Er	200	360 ± 80	0.05	4.3 ± 1.9
Tm	200	260 ± 80	0.05	2.2 ± 1.4
Yb	200	110 ± 40	0.13	0.4 ± 0.3
		Insulator		
C	200	<50	0.15	

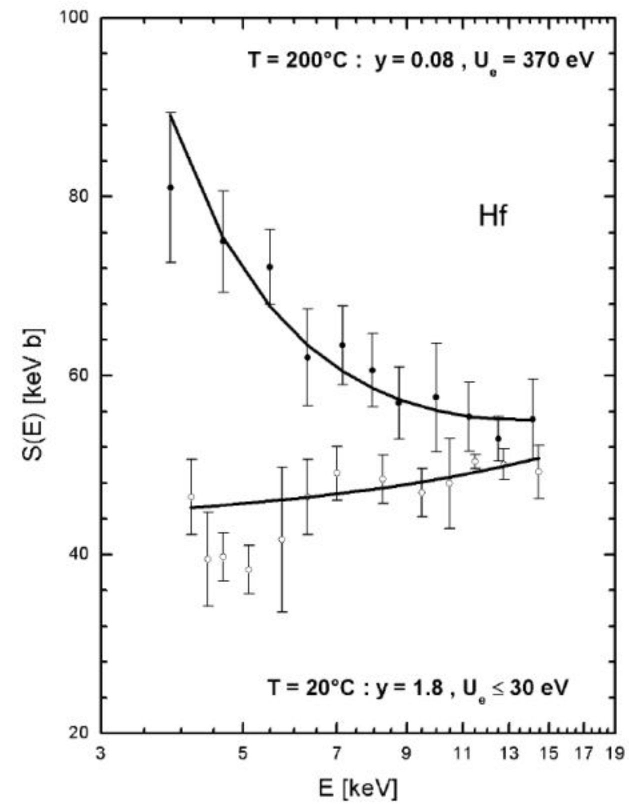

Another difficulty…

- Electron screening cannot be neglected in Nucleosynthesis calculations since all reactions occur at low energies.

Electron screening in the lab

$\neq$

Electron screening in stars

- We cannot predict the consequences of electron screening on the thermonuclear processes in stars until we first fully understand electron screening in the laboratory.

Electron Screening @ JSI

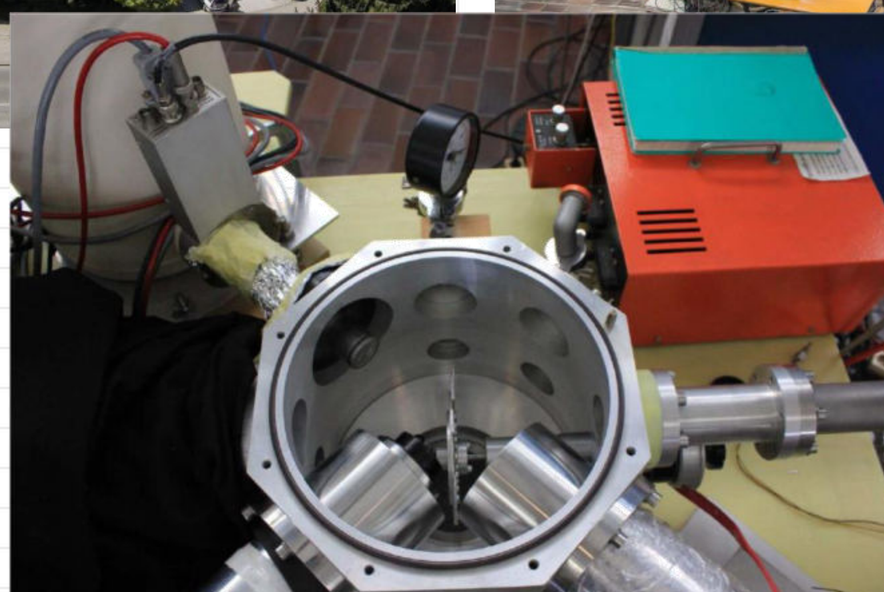

Our Previous Results

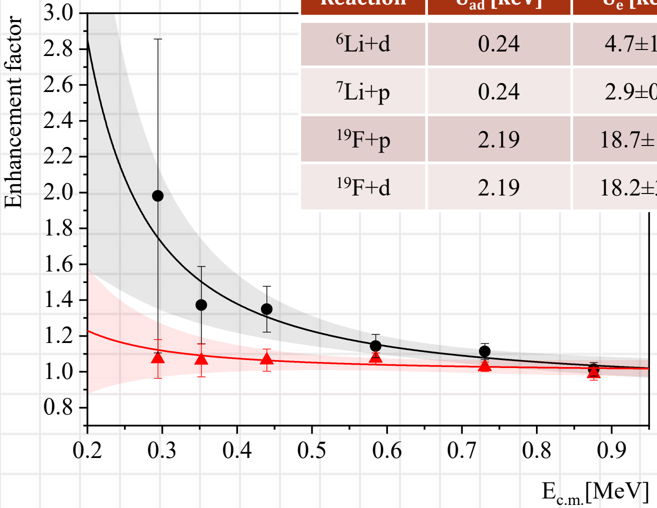

Reaction	U_{ad} [keV]	U_e [keV]
^{6}Li+d	0.24	4.7±1.3
^{7}Li+p	0.24	2.9±0.2
^{19}F+p	2.19	18.7±1.5
^{19}F+d	2.19	18.2±3.3

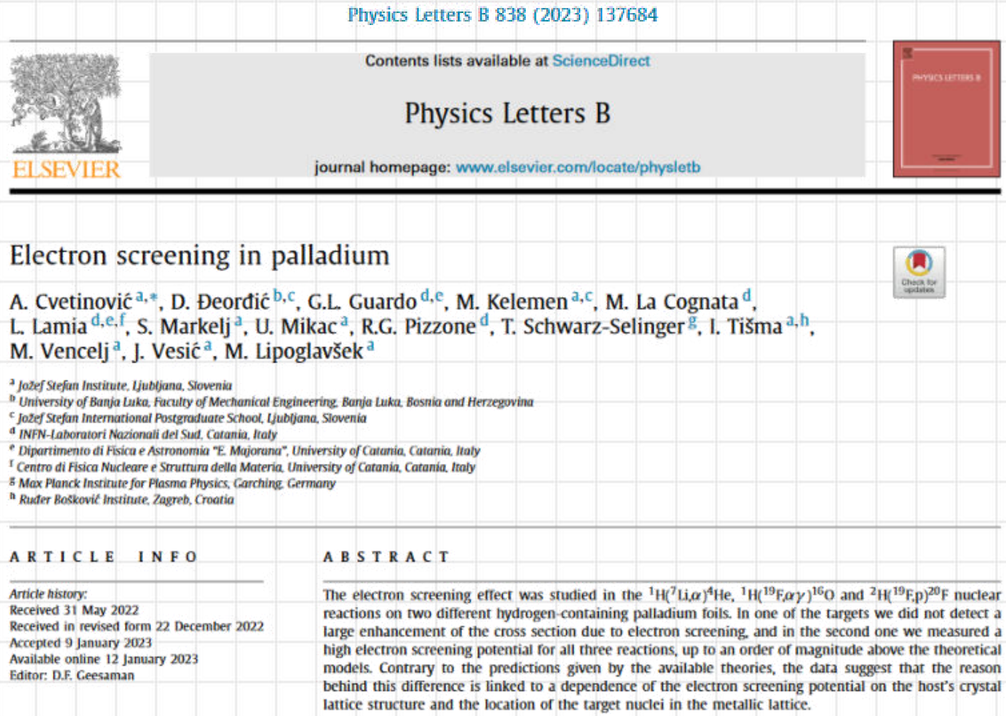

Physics Letters B 838 (2023) 137684

Contents lists available at ScienceDirect

Physics Letters B

journal homepage: www.elsevier.com/locate/physletb

ELSEVIER

Electron screening in palladium

A. Cvetinović[a,*], D. Đeorđić[b,c], G.L. Guardo[d,e], M. Kelemen[a,c], M. La Cognata[d], L. Lamia[d,e,f], S. Markelj[a], U. Mikac[a], R.G. Pizzone[d], T. Schwarz-Selinger[g], I. Tišma[a,h], M. Vencelj[a], J. Vesić[a], M. Lipoglavšek[a]

[a] Jožef Stefan Institute, Ljubljana, Slovenia
[b] University of Banja Luka, Faculty of Mechanical Engineering, Banja Luka, Bosnia and Herzegovina
[c] Jožef Stefan International Postgraduate School, Ljubljana, Slovenia
[d] INFN-Laboratori Nazionali del Sud, Catania, Italy
[e] Dipartimento di Fisica e Astronomia "E. Majorana", University of Catania, Catania, Italy
[f] Centro di Fisica Nucleare e Struttura della Materia, University of Catania, Catania, Italy
[g] Max Planck Institute for Plasma Physics, Garching, Germany
[h] Ruđer Bošković Institute, Zagreb, Croatia

ARTICLE INFO

Article history:
Received 31 May 2022
Received in revised form 22 December 2022
Accepted 9 January 2023
Available online 12 January 2023
Editor: D.F. Geesaman

ABSTRACT

The electron screening effect was studied in the $^1H(^7Li,\alpha)^4He$, $^1H(^{19}F,\alpha\gamma)^{16}O$ and $^2H(^{19}F,p)^{20}F$ nuclear reactions on two different hydrogen-containing palladium foils. In one of the targets we did not detect a large enhancement of the cross section due to electron screening, and in the second one we measured a high electron screening potential for all three reactions, up to an order of magnitude above the theoretical models. Contrary to the predictions given by the available theories, the data suggest that the reason behind this difference is linked to a dependence of the electron screening potential on the host's crystal lattice structure and the location of the target nuclei in the metallic lattice.

- Dependence on projectile Z number is ~ Z^2 instead of expected linear dependence.
- Largest electron screening in inverse kinematics, while in forward kinematics no large electron screening, except for the p+d reaction.
- Target preparation may influence electron screening, pointing to a dependence of the enhancement factor on the position of the target nuclei in the metallic lattice and electron densities around the target nucleus.
- These findings cannot be explained by the available model and theory based on static electron densities.

Electron Screening @ JSI:

Preparations for experiments

- **Goal: to find two targets with different U_e**
- **H or D containing targets:**
  - Pd, Ti, Zr, aCH, aCD
  - PdHx system does not behave like a stoichiometric compound but like a homogeneous alloy.

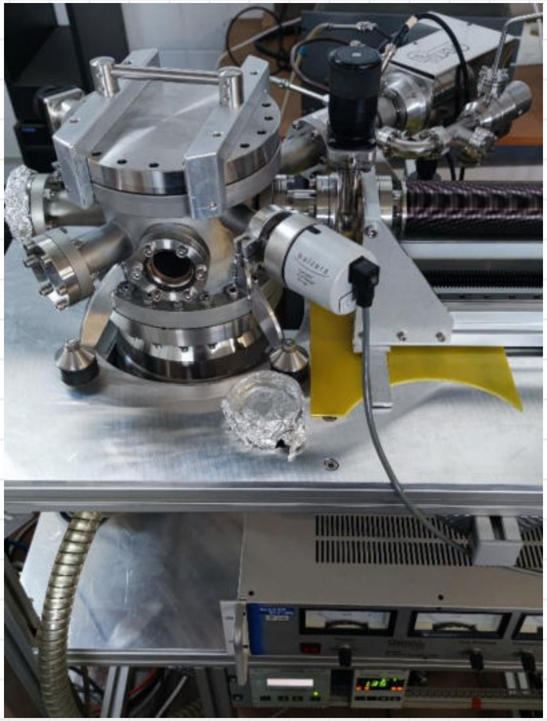

Targets implanted with ion gun:

- Extraction voltage: 3.5 kV for 24 h
- Passive cooling with copper holder

Gas loaded Pd targets:

- At room temperature and 1atm for 24 h
- **Gas mixture:** 85% D and 15% H
  - **Soft Pd:** 70% of H(D) per metallic atom (Chempur, ANNEALED)
  - **Hard Pd:** 47% of H(D) per metallic atom (Zlatarna Celje, COLD ROLLED)

Deuterium depth distribution

- Quantitative depth profiling of deuterium with the **Nuclear Reaction Analysis (NRA)**
- High-energy protons from the **$^{2}H(^{3}He,p)^{4}He$** reaction were measured at seven beam energies from **0.629** to **4.297 MeV**.

$$N_p = N_{beam}\,\overset{?}{n_D}\,\frac{\rho N_A}{M}\int_{E_0}^{0} \varepsilon\omega\,\frac{\sigma(E)}{\mathrm{d}E_{Li}/\mathrm{d}x}\,\mathrm{d}E_{He}$$

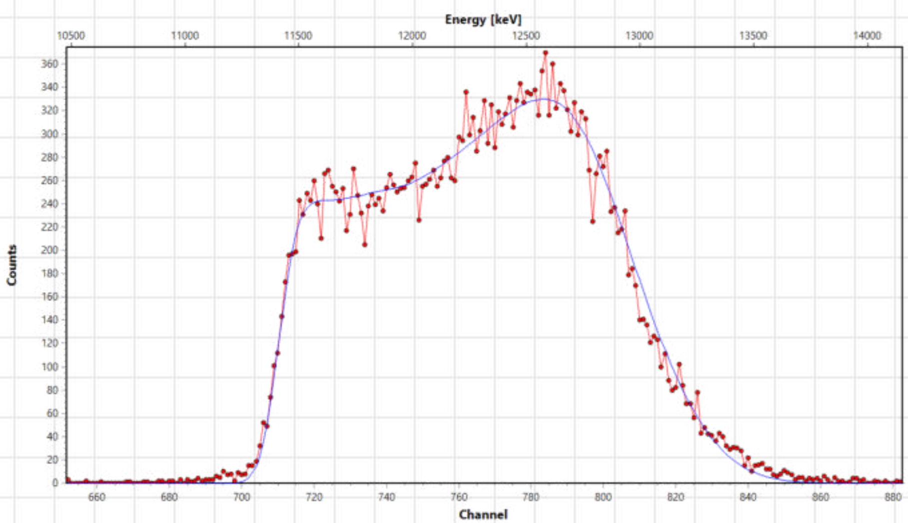

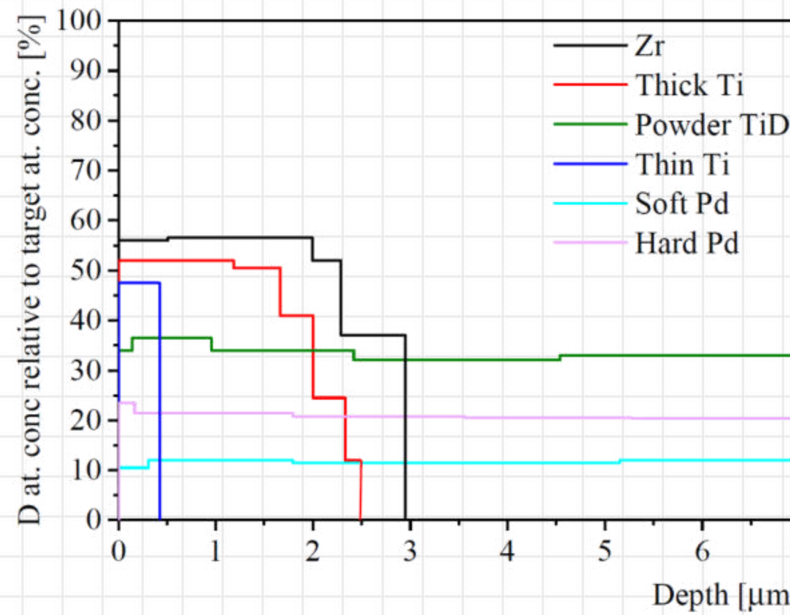

Electron Screening @ JSI:

Hydrogen in Palladium – gravimetric measurements

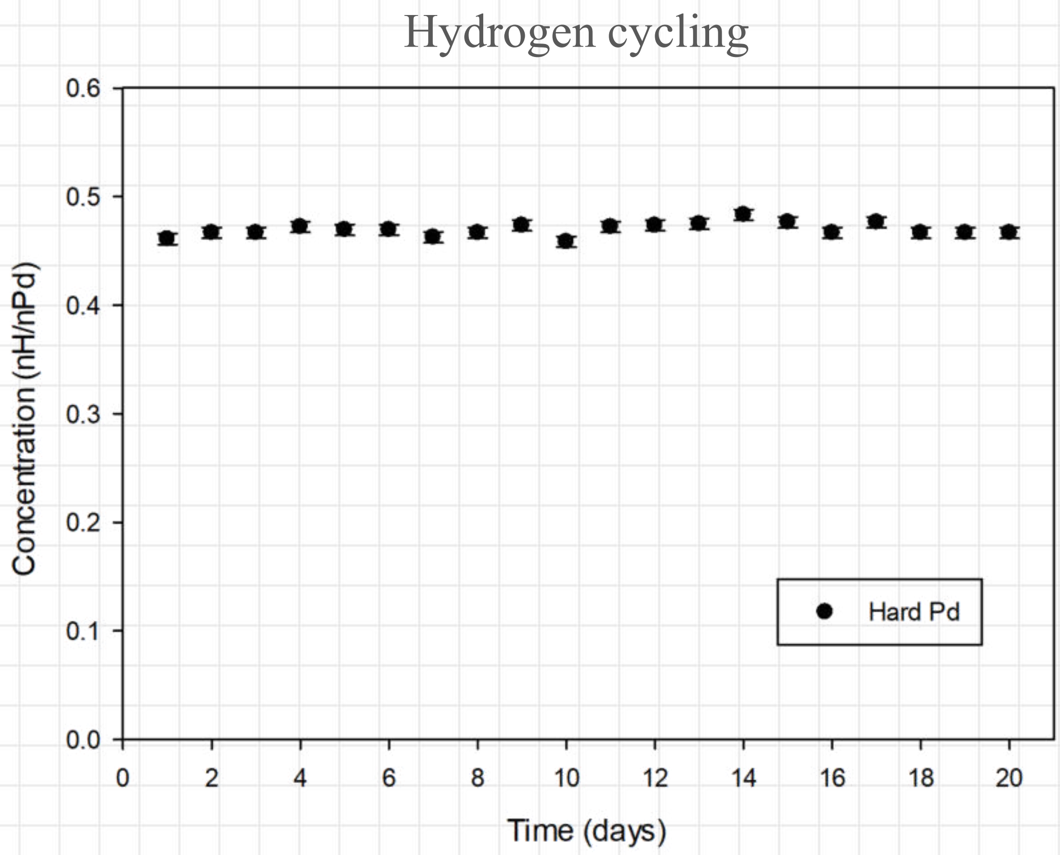

Electron Screening @ JSI:

Experimental setup

- 2-MV Tandetron accelerator at Jožef Stefan Institute
- Employed method: inverse kinematics

- „*Z*“ dependence of e.s.
- Isotopic dependence of e.s.

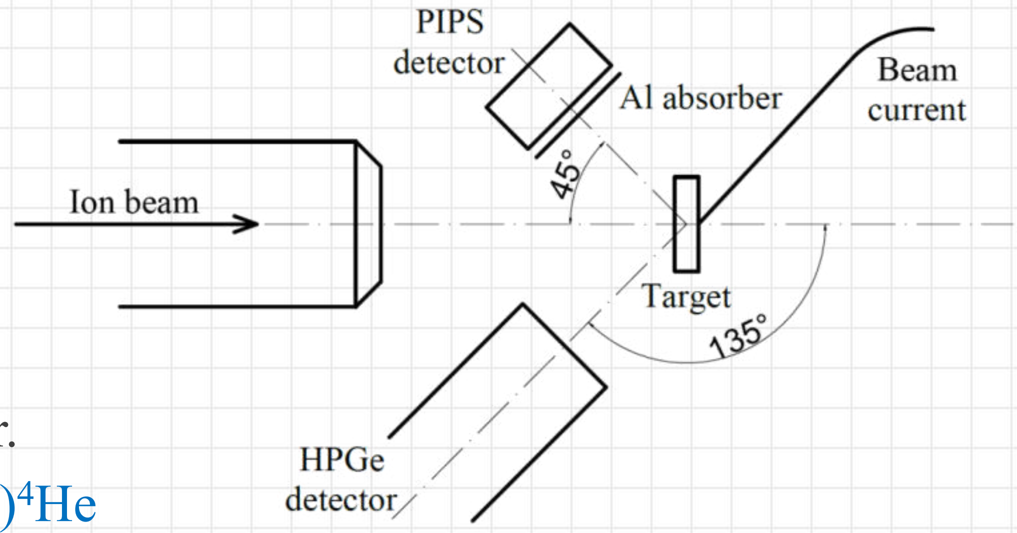

nonresonant r.	resonant r.
$^{1}H(^{7}Li,\alpha)^{4}He$	$^{1}H(^{11}B,\alpha\alpha)^{4}He$
$^{2}H(^{6}Li,\alpha)^{4}He$	$^{1}H(^{19}F,\alpha\gamma)^{16}O$
$^{2}H(^{6}Li, p_0/p_1)^{7}Li$	
$^{2}H(^{19}F,p)^{20}F \xrightarrow{\beta-} {}^{20}Ne+\gamma$	

Electron screening in Lithium

- $^{7}Li + {}^{1}H \rightarrow {}^{8}Be^{*} \rightarrow {}^{4}He + {}^{4}He$
- $^{6}Li + {}^{2}H \rightarrow {}^{8}Be^{*} \rightarrow {}^{4}He + {}^{4}He$

  $\rightarrow {}^{7}Li + p_{0}$

  $\rightarrow {}^{7}Li + p_{1} + \gamma$

^{7}Li level sheme

https://www.nndc.bnl.gov

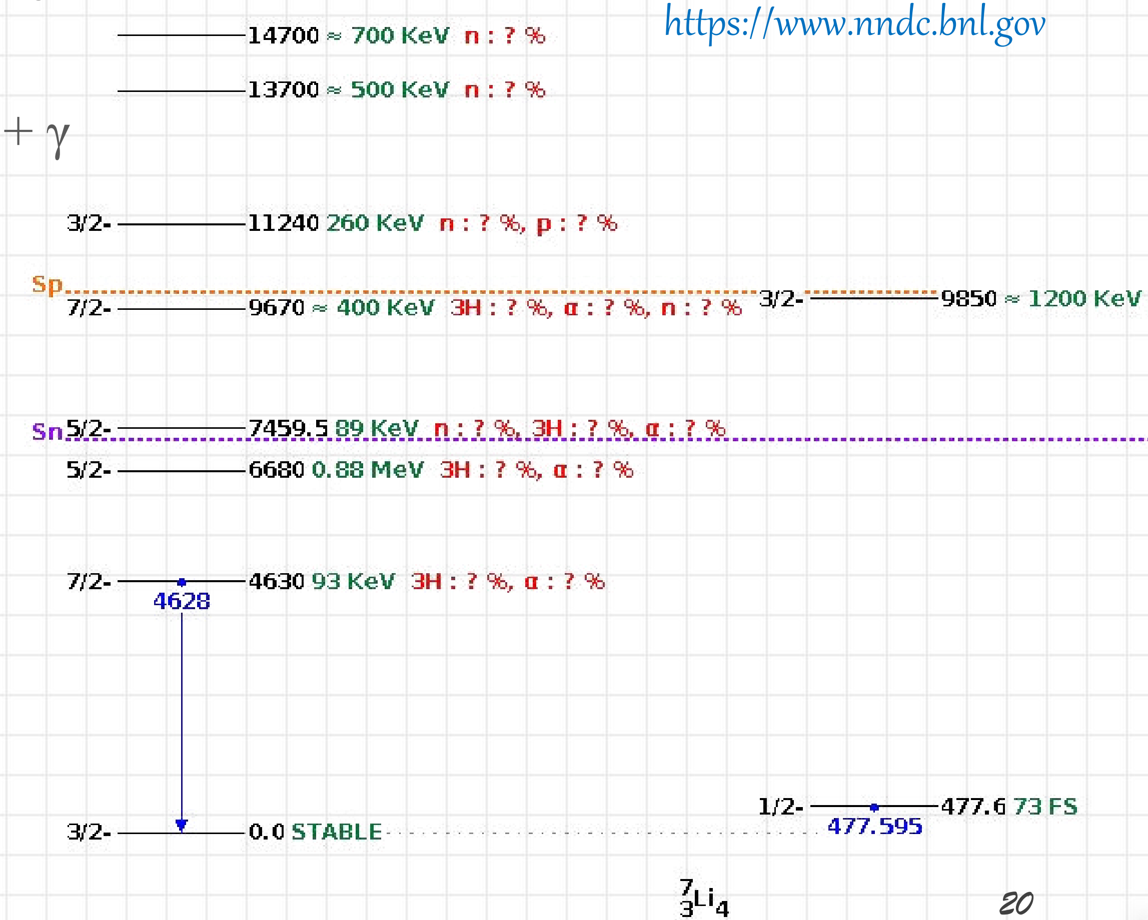

Latest Results:

$^{2}H(^{6}Li,\alpha)^{4}He$ and $^{1}H(^{7}Li,\alpha)^{4}He$

$U_{ad} = 0.24\ keV$

$$f(E) = \frac{\sigma_s(E + Ue)}{\sigma_b(\mathrm{E})}$$

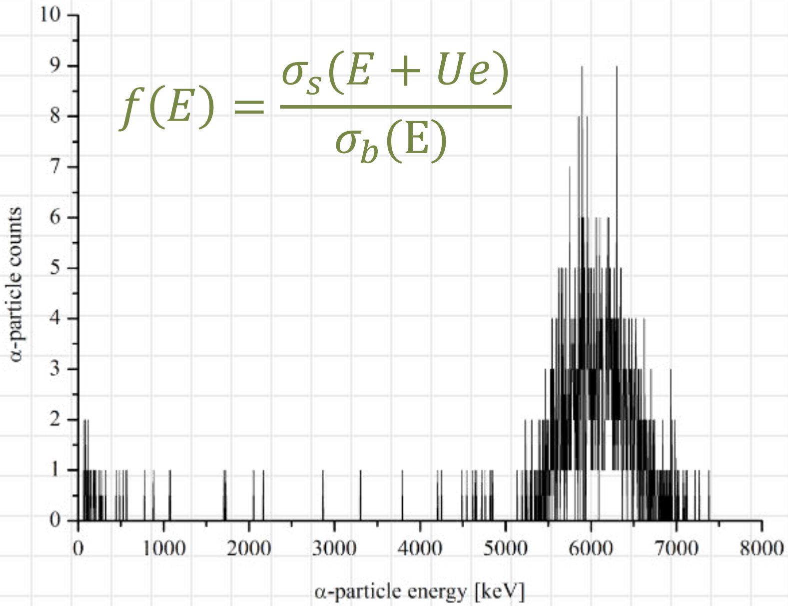

C. Spitaleri et al., Phzys. Rev. C 63, 055801 (2001).

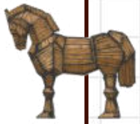

Enhancement factor:

$^{6}Li+D \rightarrow {}^{7}Li+p_0/p_1$

Latest Results:

$^6Li+D \rightarrow {}^7Li+p_0/p_1$

- J^π of particles in the entrance channel (both ^{6}Li and D) = 1^+
- J^π of the ground state of ^{7}Li = $3/2^-$
- J^π of the 1st exited state of ^{7}Li = $1/2^-$

- p_0 - no orbital angular momentum
- p_1 - orbital angular momentum =1

- $V_{Coulomb}$ = 1.9 MeV
- Q-value = 5 MeV
- $V_{Centrifugal}$ = 10 MeV

^{7}Li level sheme
https://www.nndc.bnl.gov

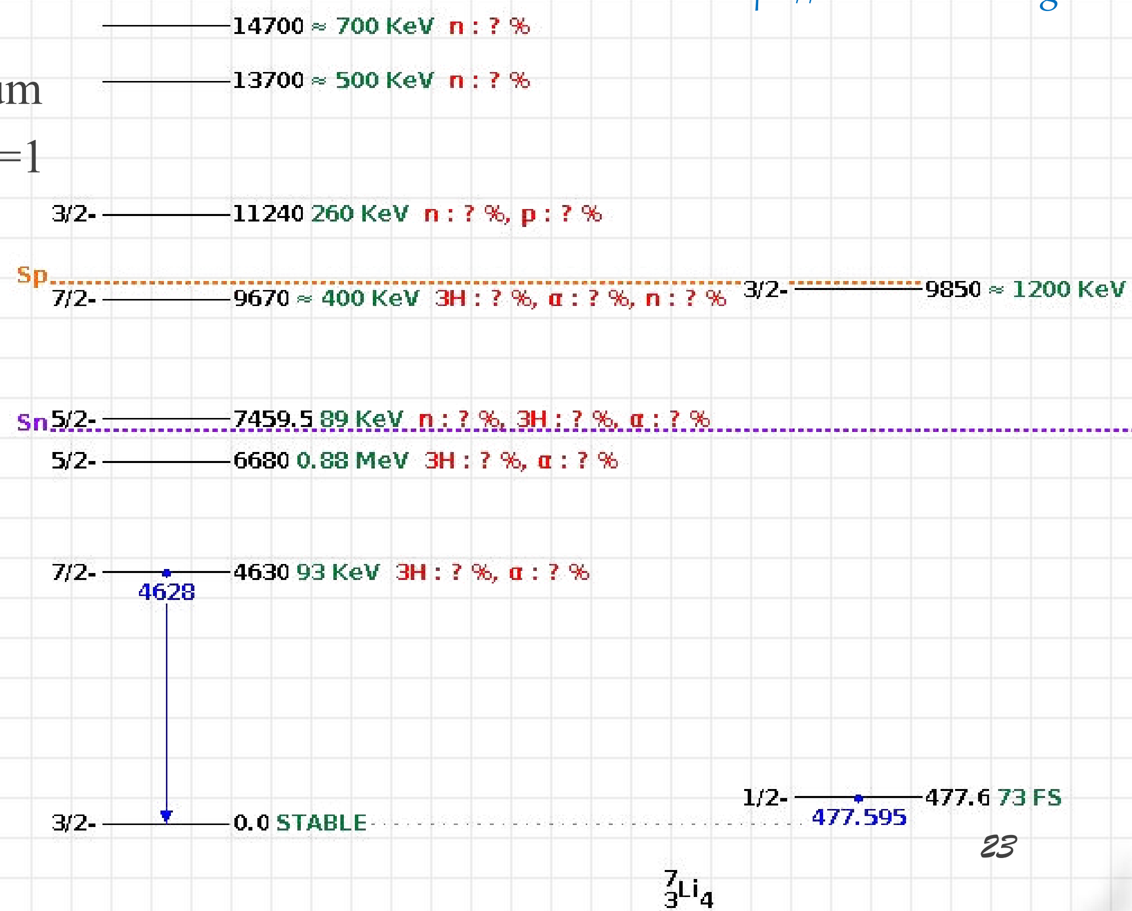

Bare-nucleus cross-section:

The ^{19}F+D reaction

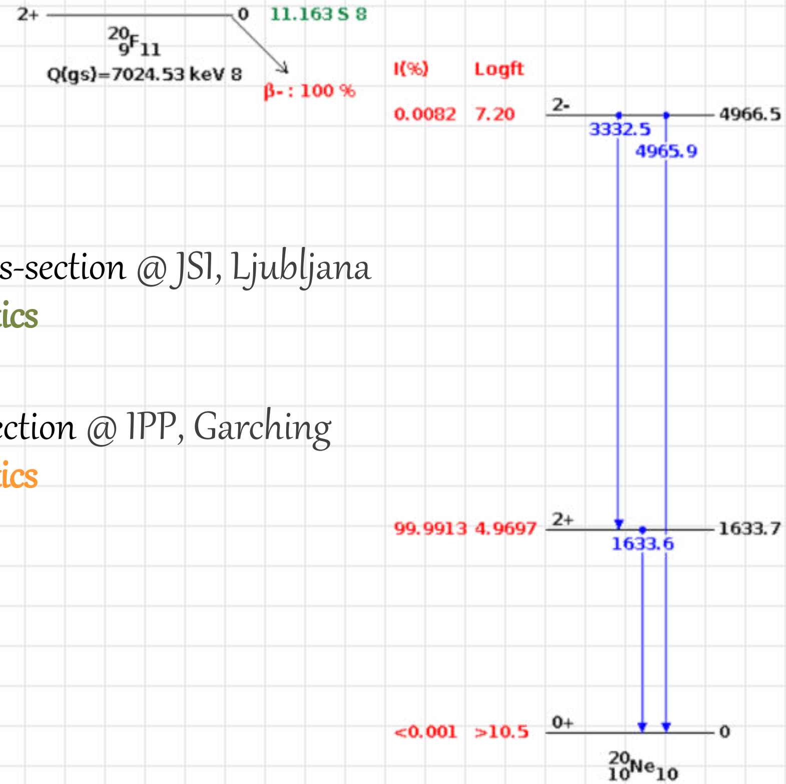

Enhancement factor:

$$f(E) = \frac{\sigma_s(E+U_e)}{\sigma_b(E)}$$

Screened-nucleus cross-section @ JSI, Ljubljana

Inverse kinematics

Bare-nucleus cross-section @ IPP, Garching

Forward kinematics

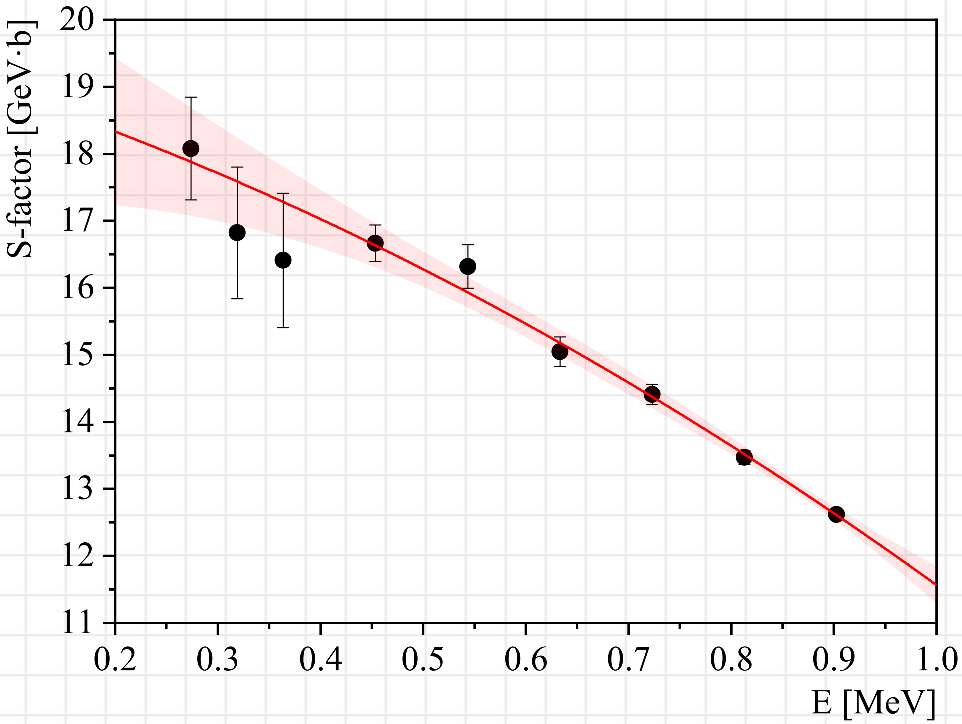

- The ^{19}F(d,p)^{20}F reaction
- ~100 nm thick CaF_2 target
- Deuterium beam

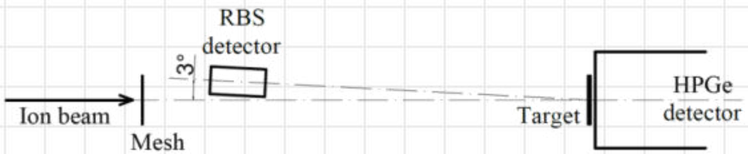

Bare-nucleus cross-section:

The ^{19}F+D reaction

Latest Results:

Resonant reactions

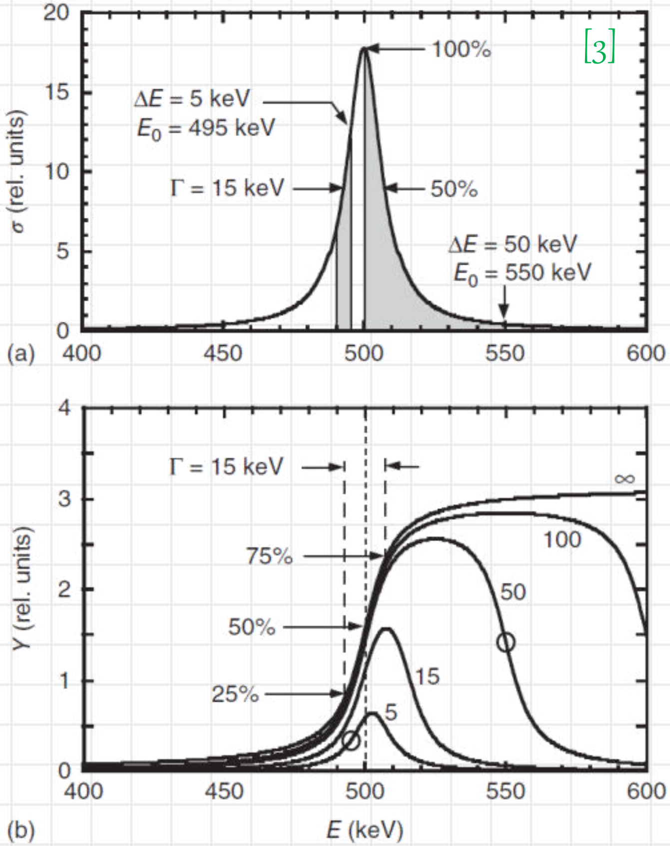

[3] C. Iliadis. Nuclear Physics of Stars - Second, Revised and Enlarged Edition, Wiley-VCH, Weinheim, 2015.

Breit-Wigner resonance cross section:

$$\sigma(E) = \frac{\lambda^2}{4\pi}\frac{\omega\gamma\Gamma}{(E_r - E)^2 + (\Gamma/2)^2}$$

$$\sigma(E_r) = \frac{\lambda^2}{2\pi}\frac{\omega\gamma}{\Gamma}$$

Enhancement factor:

$$f(E) = \frac{\sigma_s}{\sigma_b} = \frac{\omega\gamma_s}{\omega\gamma_b}$$

$\omega\gamma$ - resonance strength (= integrated cross section over resonant region)

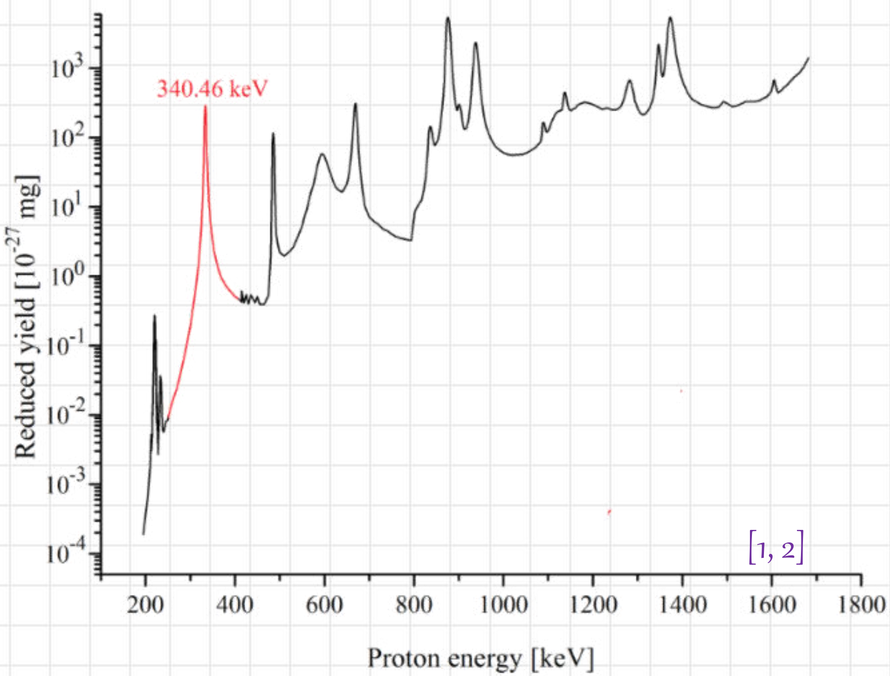

[1] K. Spyrou et al., Z. Phys., A **357**, 283 (1997).
[2] K. Spyrou et al., Eur. Phys. J., A **7**, 79 (2000).

Latest Results:

The $^{1}H(^{19}F,\alpha\gamma)^{16}O$ reaction

Thick target yield [1] :

$$Y(E) = \frac{\lambda^2}{2\pi}\frac{\omega\gamma}{\varepsilon_r^{eff}}\left[\arctan\left(\frac{E-E_r}{\Gamma/2}\right) - \arctan\left(\frac{E-E_r-\Delta E}{\Gamma/2}\right)\right]$$

[1] C. Iliadis. Nuclear Physics of Stars, 2015.
[2] K. Spyrou et al. Eur. Phys. J., A 7:79, 2000.

Latest Results:

The $^{1}H(^{11}B,\alpha\alpha)^{4}He$ reaction

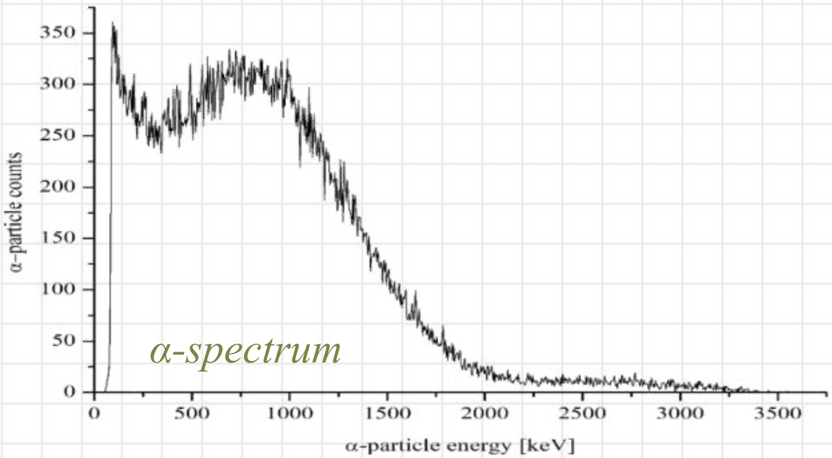

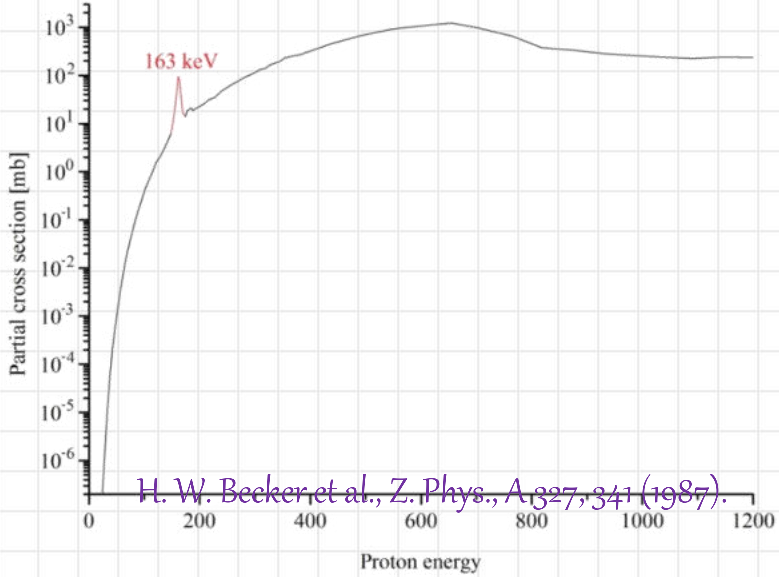

Target analysis:

Nuclear Magnetic Resonance and Knight shift

- The Knight shift originates from the interaction of conducting electrons in metals with nuclear spins and is proportional to the density of electronic states at the Fermi level at the nucleus site

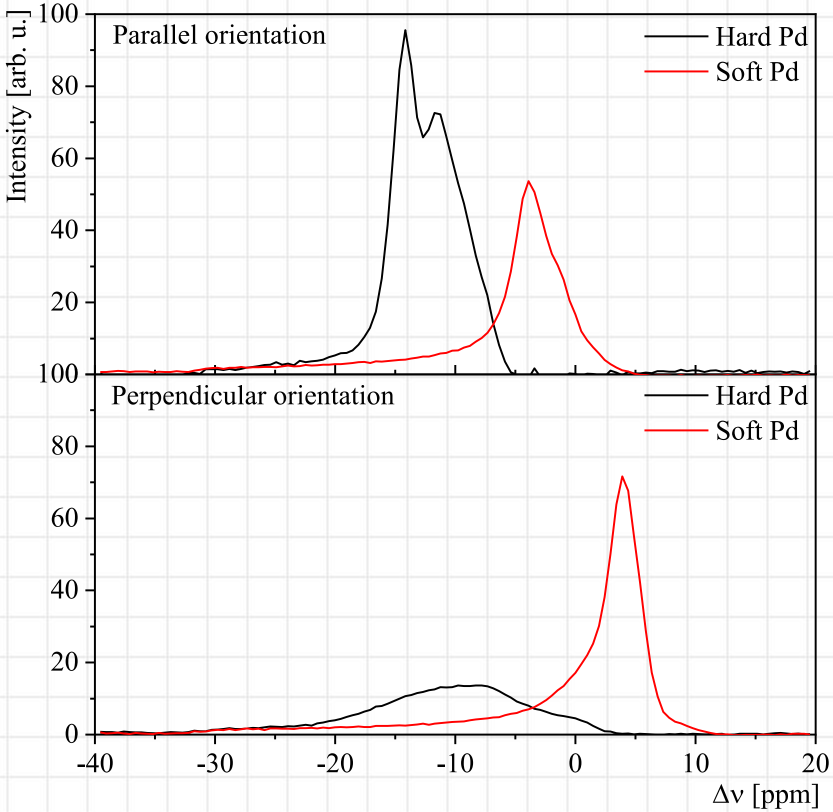

Foil	n_D	K_{H_1} [ppm]	K_{H_2} [ppm]	K_{H_t} [ppm]
Soft Pd	0.70	26.7	/	≈18
Hard Pd	0.47	20.2	15.6	≈-14

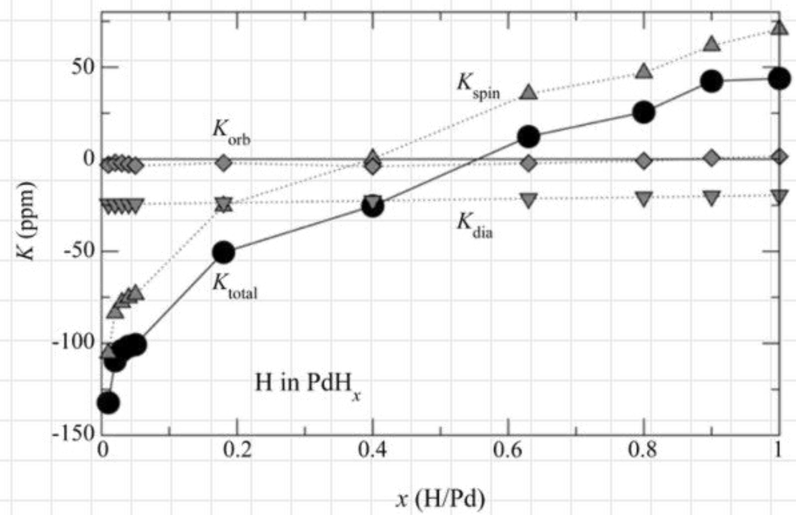

The theoretical Knight shift of H in PdHx over the entire range of x [M. Deng et al. Solid State Communications, 150:1262, 2016.].

A. Cvetinović et all., Phys. Lett. B, 838 (2023), 137684

Latest Results:

Crystal symmetry

H located at regular octahedral interstitial sites

small screening

H trapped at grain boundaries, dislocations and voids

large screening

fcc (Pd)

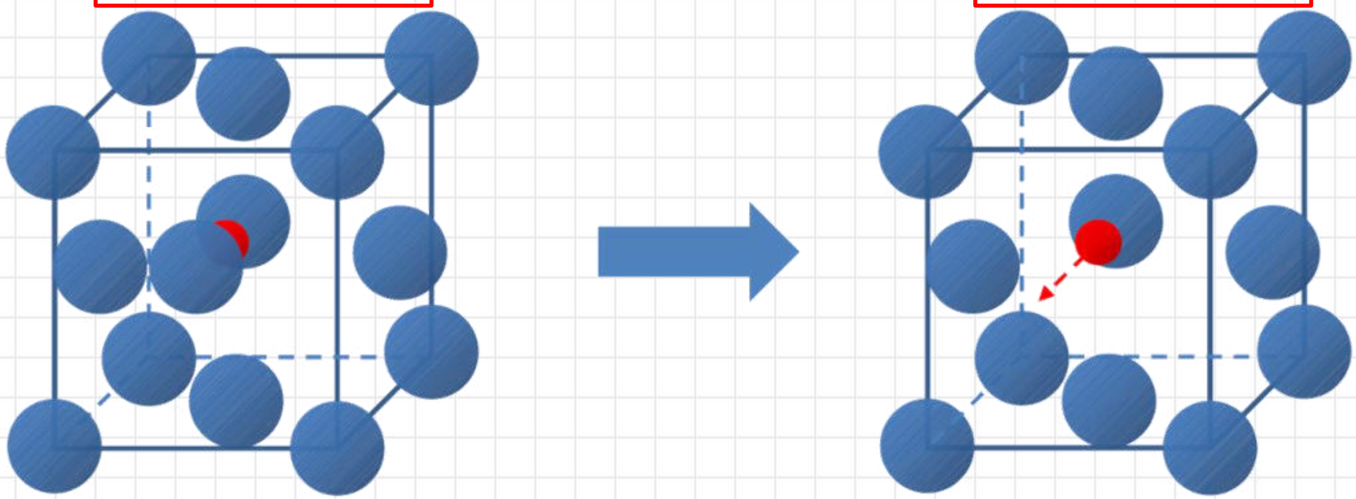

Conclusions

- Contrary to the predictions given by the Adiabatic model, the large electron screening is not linked to the static electron densities around interacting nuclei.
- Static picture can explain only small electron screening.
- Crystalline effects have to be considered in order to explain huge measured U_e values.
- Large screening is induced by placing the target nuclei at specific positions in crystal lattice where the density of electronic states is higher.
- Connection between metals and plasma is still not understood!

Thank you for your atention!